Technical Physics, 2025, Vol. 70, No. 3

01

Simulation of the ultra-short pulses dynamics in a polymer composite with graphene nanoribbons and metal nanoparticles

© N.N. Konobeeva

Volgograd State University,
400062 Volgograd, Russia
e-mail: yana_nn@volsu.ru

Received November 21, 2024
Revised November 21, 2024
Accepted November 21, 2024

In this paper, we study the evolution of a short-duration two-dimensional and three-dimensional electromagnetic pulse when it interacts with a composite of a polymer and graphene nanoribbons containing metal nanoparticles (atoms adsorbed on the graphene surface). Based on the wave equation, taking into account the contributions of the nanoribbons and polymer to the current, an effective equation for the vector potential of the electric field of the pulse is obtained. It is found that the introduction of metal adatoms into the polymer matrix causes a change in the amplitude of the wave propagating in such a system. The parameters of the electromagnetic wave are analyzed depending on the pulse type (two-dimensional and three-dimensional), the type of metal particle, and the concentration of the polymer in the composite.

Keywords: polymer composite, graphene nanoribbons, metal nanoparticles, electromagnetic pulses.

DOI: 10.61011/TP.2025.03.60847.419-24

Introduction

In recent decades, the unique properties of carbon-based nanostructures have been used actively in entirely different areas of scientific research and advanced technology (semiconductor, optoelectronic, etc.). Specifically, one of the priority tasks in nonlinear optics is the selection of a material that would provide certain desired parameters of electromagnetic pulses. Carbon nanotubes (CNTs) [1,2] and other graphene-like materials (graphene ribbons, silicene, germanene) [3] are promising candidates in this context. For example, the possibility of stable propagation of pulses containing several oscillations of the electromagnetic field (in most cases, 1–3 oscillations; such pulses are often called extremely short ones, ESPs) in such structures was demonstrated in [4,5]. This is achieved due to the balance of dispersion and nonlinearity of the system. It was demonstrated that the magnitude of spin-orbit interaction has a significant influence on the evolution of ESPs.

A pressing problem in this case is the determination of purity of a material, which often contains various inclusions, including metal (platinum, gold, silver, etc.) nanoparticles. The physical and chemical properties of nanoparticles differ from those of the materials from which they were obtained. A large number of metal and metal oxide nanoparticles have already been synthesized, and their unique electrical, magnetic, optical, and catalytic properties make them sought-after in various fields of science and technology. Specifically, they may be used separately or in combination with other nanostructures in biosensors to enhance the signal, raise the sensitivity and detectivity, and perform quantitative determination of various biomolecules [6]. Hybrids of noble metal nanoparticles and carbon nanotubes are used as electrocatalysts for fuel cells [7]. It is worth noting that such impurities may alter the energy spectrum of carbon nanostructures [8,9] and, consequently, their properties; in general, they exert both a positive influence and a negative one. This is what makes the study of this influence on the characteristics of a pulse important.

The use of carbon nanomaterials in the design of various optoelectronic components, including ultra-compact optoelectronic filters [10], optoelectronic integrated circuits [11], photonic emitters [12], etc., is also worthy of note.

In the present study, we examine the dynamics of a short-duration infrared laser pulse interacting with a polymer composite with graphene nanoribbons [13] that contain metallic impurities. A model developed earlier, which needs to be modified to factor in the presence of polymers in the medium, is used for calculations.

Nanoribbons are quasi-one-dimensional materials with a honeycomb structure with a width of several atoms [14]. From an application point of view, a variety of methods for synthesis of a large number of two-dimensional monolayer materials are available at present. Different types of nanoribbons, such as silicene, boron nitride, gallium oxide, graphene ones, etc., have already been examined in detail. The present study is focused on graphene nanoribbons [15], which are a monolayer of sp^2-hybridized carbon atoms arranged in two-dimensional lattices with an aspect ratio of more than one hundred that have significant interphase regions and edge regions. As for the methods of production of graphene nanoribbons, two main approaches may be distinguished: top-down synthesis and bottom-up synthesis, which include chemical techniques, plasma etching, lithography, etc. [16,17]. In addition to graphene processing, CNT unwrapping is also used [18].

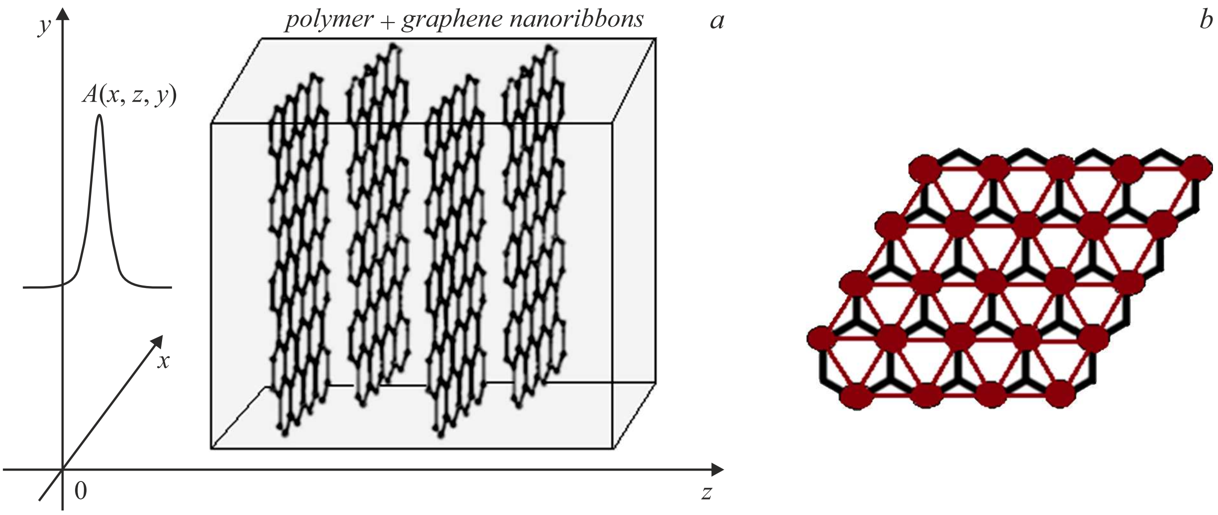

Figure 1. *a* — schematic diagram of the system geometry; *b* — fragment of a graphene nanoribbon with a layer of metal particles, which are represented by red circles (top view); red lines indicate the bonds between metal adatoms.

Graphene nanoribbons have a variety of practical applications; however, since graphene has no band gap, it cannot be used in optoelectronic devices [19]. One of the methods for increasing the band gap is doping with various types of impurities, including metallic ones.

It is worth noting that the use of the composite is made feasible by the need to obtain a given geometry of graphene nanoribbons with a specific orientation and distances between them. This may be achieved both in the process of formation of the composite and after the introduction of nanoribbons into the polymer matrix with the application of such external inputs as electric and magnetic fields, mechanical deformation (compression and stretching), or catalysts [20–23]. It has been demonstrated numerous times that graphene nanoribbons may be aligned in a polymer matrix to form composites. It was found that such hybrid forms have better mechanical strength, electrical conductivity, thermal stability, and rheological characteristics.

Note also that the evolution of electromagnetic pulses in CNTs with polymers (thin composite films [26] included, although without metallic impurities) in two-dimensional [24] and three-dimensional [25] cases has already been studied. Therefore, in the present study, we focus on the effects that manifest themselves in the behavior of an extremely short pulse and are caused by the presence of metal nanoparticles (atoms adsorbed on the graphene surface) in a composite of graphene nanoribbons with a polymer; in other words, we examine the influence of metal adatoms on the pulse characteristics.

1. Model and basic equations

Let us consider the propagation of an extremely short optical pulse in a medium with a polymer containing graphene nanoribbons with zigzag-type boundaries. The composite material is positioned in the path of the laser pulse in such a way that the electric field strength vector and vector potential $\mathbf{A}(x, z, t)$ are directed at an angle of 90° to the nanoribbon plane (Oy), while the wave vector is oriented parallel to axis Oz (Fig. 1). Note that nanoribbons are assumed to be single-layer in our model. Such ribbons may be obtained, e.g., by electron lithography, wherein graphene is cut into pieces [27], or from two-layer CNTs unzipping in the process of ultrasonic treatment [28]. We examine the adsorption of nickel and copper atoms on a graphene nanoribbon with metal particles forming a single layer of closely packed adatoms. Notably, nickel adatoms interact strongly with a graphene nanoribbon (stronger hybridization), while copper adatoms interact weakly. The structure of nanoribbons is regular without deformations; defects are induced by the presence of metallic impurities, which leads to a change in the Hamiltonian parameters.

The Hamiltonian characterizing the electronic properties of a graphene nanoribbon takes the form [29,30]

$$H = H_{\mathrm{kin}} + H_{\mathrm{pot}} + H_{\mathrm{int}} + H_{\mathrm{R}}, \tag{1}$$

where H_{kin} is the kinetic energy of electrons, H_{pot} is the potential energy, H_{int} is the exchange interaction, and H_{R} is the Rashba spin-orbit interaction. The constituent parts of the Hamiltonian are

$$\begin{aligned}
&H_{\mathrm{kin}} = \hbar v_{\mathrm{D}}(\tau k_x \sigma_x + k_y \sigma_y),\\
&H_{\mathrm{pot}} = \Delta_{bg} \sigma_z s_0,\\
&H_{\mathrm{int}} = \lambda_A \frac{\sigma_z + \sigma_0}{2} s_z + \lambda_B \frac{\sigma_z - \sigma_0}{2} s_z,\\
&H_{\mathrm{R}} = \lambda_R(\tau \sigma_x s_y - \sigma_y s_x),
\end{aligned} \tag{2}$$

where k_x, k_y are the electron wave function components; v_{D} is the velocity of electrons in the vicinity of the Dirac point; $\tau = \pm 1$ with account for the valley sign for Dirac points; Δ_{bg} is the band gap half-width; λ_A, λ_B are the exchange interaction constants for sublattices A and B of a two-dimensional graphene sheet; λ_{R} is the Rashba spin-orbit interaction constant; σ_i $(i = x, y, z)$, s_i $(i = x, y, z)$ are the Pauli matrices in spin and lattice spaces; and σ_0, s_0 are unit matrices in the corresponding spaces.

The chosen values of the interaction constants of Hamiltonians H_{int} and H_{R} and the Δ_{bg} value corresponded to the case when a metal adatom is located above a carbon atom of sublattice A. Therefore, the coupling with this sublattice is assumed to be stronger compared to that with sublattice B. It is known that the Rashba spin-orbit interaction constant for the graphene plane is close to zero; however, an energy gap opens in the spectrum when impurities are present, and λ_{R} increases significantly [31].

Total energy operator (1) was then presented in matrix form:

$$H = \begin{pmatrix} \alpha & 0 & a & b \\ 0 & \beta & s & a \\ a^* & s^* & \gamma & 0 \\ b^* & a^* & 0 & \delta \end{pmatrix},$$

$$\alpha = \Delta_{bg} + \lambda_A, \;\; \beta = \Delta_{bg} - \lambda_A,$$
$$\gamma = -\Delta_{bg} - \lambda_B, \;\; \delta = -\Delta_{bg} - \lambda_B,$$
$$a = \hbar v_{\mathrm{D}}(\tau k_x - i k_y), \;\; b = i\lambda_{\mathrm{R}}(1 - \tau),$$
$$s = i\lambda_{\mathrm{R}}(1 + \tau) \qquad (3)$$

and the eigenvalue problem was solved using the Descartes–Euler method [32]:

$$\varepsilon_{1,2,3,4} = \sqrt{z_1} \pm \sqrt{z_2} \pm \sqrt{z_3},$$
$$z_i = w_i - \frac{p}{6}, \quad w_1 = M_1 + M_2,$$
$$w_{2,3} = -\frac{M_1 + M_2}{2} \pm i\sqrt{3}\,\frac{M_1 - M_2}{2},$$
$$M_1 = \sqrt[3]{-0.5q_1 + \sqrt{Q_1}}, \;\; M_2 = \sqrt[3]{-0.5q_1 - \sqrt{Q_1}},$$
$$Q_1 = \left(\frac{p_1}{3}\right)^3 + \left(\frac{q_1}{2}\right)^2, \;\; p_1 = -\frac{p^2}{12} + \frac{p^2 - 4r}{16},$$
$$q_1 = \frac{p}{6}\left(\frac{p^2}{18} - \frac{p^2 - 4r}{16}\right) - \frac{q^2}{64},$$
$$p = -\frac{3F^2}{8} + B, \quad q = \frac{F^3}{8} - \frac{FB}{2} + C,$$
$$r = -\frac{3F^4}{256} + \frac{F^2 B}{16} - \frac{FC}{4} + D,$$
$$F = -(\alpha + \beta + \lambda + \delta),$$
$$B = \alpha\beta + (\alpha + \beta)(\gamma + \delta) + \gamma\delta - 2|a|^2 - |b|^2 - |s|^2,$$
$$C = -\alpha\beta(\gamma + \delta) - \gamma\delta(\alpha + \beta) + |s|^2(\alpha + \delta) + |b|^2(\beta + \gamma),$$
$$D = \alpha\beta\gamma\delta - \alpha\gamma|a|^2 - \alpha\delta|s|^2 + |a|^4 - a^2 b^* s^*$$
$$- |a|^2\beta\delta - |b|^2\beta\gamma - (a^*)^2 bs + |b|^2|s|^2. \qquad (4)$$

The equation characterizing the propagation of an extremely short pulse may be written as follows:

$$\Delta\mathbf{A} - \frac{\varepsilon_m}{c^2}\frac{\partial^2\mathbf{A}}{\partial t^2} + \frac{4\pi}{c}\mathbf{j}(\mathbf{A}) = 0. \qquad (5)$$

Here, $\mathbf{A}$ is the vector potential of the electric field, c is the speed of light, ε_m is the permittivity of the medium, $\mathbf{j}$ is the electric current density, and Δ is the Laplace differential operator.

In the present study, we consider the two-dimensional case with vector potential assuming the form $\mathbf{A} = \big(0, A(x, z, t), 0\big)$; therefore, the current density will have only one non-zero y component.

Since the polymer matrix is a composite of a polymer with graphene nanoribbons, the current density has two components:

$$j(A) = j_1(A) + j_2(A), \qquad (6)$$

where j_1, j_2 are the contributions of graphene nanoribbons and polymers to the electric current, respectively.

In the low-temperature approximation, the expression for current density j_1 is written as

$$j_1 = e\int_{-h}^{h}\int_{-h}^{h} dp_x dp_y\, v_y\left(p_x, p_y - \frac{e}{c}A(x, z, t)\right),$$

$$v_y(p_x, p_y) = \partial E(p_x, p_y)/\partial p_y, \qquad (7)$$

where $v_y(p_x, p_y)$ is the velocity of electrons; p_x, p_y are the electron momentum components; e is the electron charge; and $E(p_x, p_y)$ is the electron dispersion law determined according to expression (4).

Limits of integration h over a rectangular region are determined based on the equality of the number of particles that follows the Fermi–Dirac distribution:

$$\int_{-h}^{h}\int_{-h}^{h} dp_x dp_y = \iint_{1^{\mathrm{st}}BZ} dp_x dp_y \langle a^+_{p_x,p_y}, a_{p_x,p_y}\rangle, \qquad (8)$$

where $1^{\mathrm{st}}BZ$ denotes the first Brillouin zone; $a^+_{p_x,p_y}$, a_{p_x,p_y} are the creation and annihilation operators for electrons; and $\langle \ldots \rangle$ denotes averaging with the density operator.

The second component of current density j_2 was calculated similarly to the calculation of current in a system of quantum dots with hopping conductivity [33]. This model was detailed and validated for polyacetylene in [34]:

$$j_2 = e\gamma_0 \frac{3d}{2\hbar}\chi_{\mathrm{pol}} \sin\left(\frac{a_{\mathrm{POL}} e A}{c}\right), \qquad (9)$$

$\gamma_0 = 2.7\,\mathrm{eV}$, $d = 0.142\,\mathrm{nm}$, a_{POL} — length of a carbon bond in a polymer, and χ_{pol} defines the concentration of electrons in the polymer.

2. Results of numerical modeling: two-dimensional case

The obtained Eq. (5) was solved with (7) and (9) taken into account using the finite difference numerical method [35] with standard stability conditions. The initial condition for an extremely short pulse consisting of a single field oscillation was specified in the form of a Gaussian function:

$$A(x,z,0) = Am\exp\left(-\frac{z^2}{\gamma_z^2}\right)\exp\left(-\frac{x^2}{\gamma_x^2}\right),$$

$$\frac{dA(x,z,0)}{dt} = \frac{2Am\,z\,v_z}{\gamma_z^2}\exp\left(-\frac{z^2}{\gamma_z^2}\right)\exp\left(-\frac{x^2}{\gamma_x^2}\right). \quad (10)$$

Here, Am is the pulse amplitude; $v_z = 0.95c$ is the pulse velocity at time point $t = 0$ (in units of the speed of light); and γ_z, γ_x define the pulse width in the specified directions ($6\,\mu$m and $16.5\,\mu$m).

Numerical modeling was performed with the following parameters: the polymer (polyacetylene) matrix was $1 \times 1 \times 1$ cm in size, the polymer concentration was close to 75 %, $z = 0$ corresponded to its location (origin) and the point of entry of a pulse into the composite, the approximate width of graphene nanoribbons was 20 nm, and the distance between them was $0.2\,\mu$m. The parameters of the Hamiltonian in formula (3) were as follows: for Ni nanoparticles — $\Delta_{bg} = 29.5$ meV, $\lambda_R = 4.9$ meV, $\lambda_A = 60.8$ meV, $\lambda_B = 8.9$ meV, for Cu — $\Delta_{bg} = 7.9$ meV, $\lambda_R = 1.6$ meV, $\lambda_A = 1.97$ meV, $\lambda_B = 0.16$ meV [31]. The distance between the particle layer and the graphene nanoribbon was 0.306 and 0.312 nm for Ni and Cu, respectively. The electric field strength of an extremely short pulse at the initial moment of time (maximum value) was $5 \cdot 10^7$ V/m.

The intensity of the electric field of the pulse was determined as

$$I \propto E^2,$$

$$E = -\frac{1}{c}\frac{\partial A}{\partial t}. \quad (11)$$

Figure 2 presents the variation of intensity of a two-dimensional extremely short optical pulse in the process of its propagation through the composite with graphene nanoribbons and nickel nanoparticles.

According to Fig. 2, the pulse motion is fairly localized, and the spatial shape is preserved. At the same time, the front edge is distorted significantly, and the formation of several peaks following the main one is observed.

Figure 3 illustrates the features of behavior of an extremely short optical pulse induced by different types of nanoparticles.

It can be seen that the pulse shape and the front curvature depend strongly on the presence/lack of nanoparticles. It is worth noting that the specific type of metal particles has a less significant effect on the shape of a pulse than on its intensity.

The dependence of characteristics of an extremely short pulse on the polymer concentration is shown in Fig. 4.

The obtained dependences suggest that an increase in polymer concentration in the composite leads to a stronger pulse spreading compared to propagation in a medium containing graphene nanoribbons outside of the polymer matrix. On the one hand, the use of a polymer makes it convenient to work with nanoribbons; on the other hand, it leads to more profound changes in the pulse characteristics relative to the original parameters. Therefore, this effect should be taken into account in synthesis of composites.

3. Results of numerical modeling: three-dimensional case

The wave equation for the vector potential may be written in this case in a cylindrical coordinate system:

$$\frac{\varepsilon_m}{c^2}\frac{\partial^2 A}{\partial t^2} - \frac{1}{r}\frac{\partial}{\partial r}\left(r\frac{\partial A}{\partial r}\right) - \frac{\partial^2 A}{\partial \varphi^2} - \frac{\partial^2 A}{\partial z^2} = \frac{4\pi}{c}\big(j_1(A) + j_2(A)\big),$$

$$r^2 = x^2 + y^2, \quad \varphi = \mathrm{arctg}\left(\frac{y}{x}\right). \quad (12)$$

Here, the vector potential of the momentum field is given by

$$\mathbf{A} = \big(0, A(x^2+y^2, z, t), 0\big).$$

The third term in Eq. (12) containing the second derivative with respect to angle φ may be neglected, since the smallness of the accumulated charge (according to the estimates made in earlier studies, the contribution of the accumulated charge does not exceed 2 % of the total contribution to the current value) ensures a cylindrical symmetry of the electric field of the pulse [36].

The initial condition was chosen as in the two-dimensional case (with allowance for the transition to a cylindrical coordinate system):

$$A(r^2,z,0) = Am\,\exp\left(-\frac{z^2}{\gamma_z^2}\right)\exp\left(-\frac{r^2}{\gamma_r^2}\right),$$

$$\frac{dA(r^2,z,0)}{dt} = \frac{2Am\,z\,v_z}{\gamma_z^2}\exp\left(-\frac{z^2}{\gamma_z^2}\right)\exp\left(-\frac{r^2}{\gamma_r^2}\right), \quad (13)$$

where $\gamma_z = 3\,\mu$m and $\gamma_r = 6\,\mu$m is the pulse width along coordinate r.

The dynamics of intensity variation of a three-dimensional extremely short electromagnetic pulse is presented in Fig. 5.

As in the 2D case, the pulse propagating through the sample undergoes broadening and a reduction in amplitude due to the emergence of peaks of slightly different magnitudes. Notably, its front is not distorted.

The pulse characteristics for hybrids with and without different nanoparticles were also investigated. It was found that the polymer composite with metal nanoparticles provides a more localized propagation of a three-dimensional pulse than the composite without them. An increase in the

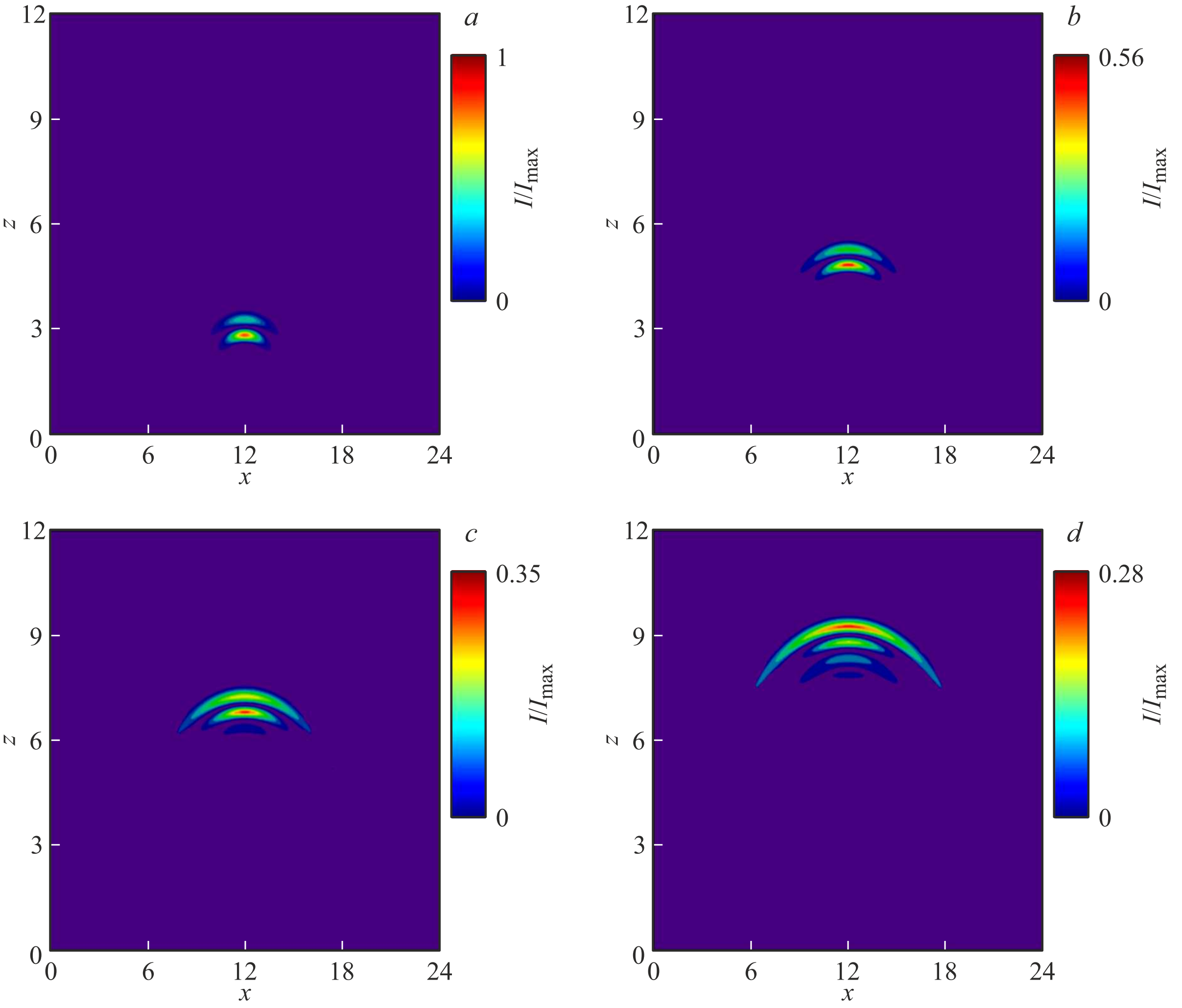

Figure 2. Intensity of the electric field of a two-dimensional electromagnetic pulse propagating through the composite with graphene nanoribbons containing nickel nanoparticles at different points in time: *a* — $t = 3.0 \cdot 10^{-13}$ s; *b* — $t = 5.0 \cdot 10^{-13}$ s; *c* — $t = 7.0 \cdot 10^{-13}$ s; *d* — $t = 9.0 \cdot 10^{-13}$ s. The coordinate scales units correspond to $2 \cdot 10^{-5}$ m. The color scale represents the intensity normalized to the maximum level for all panels (*a*–*d*).

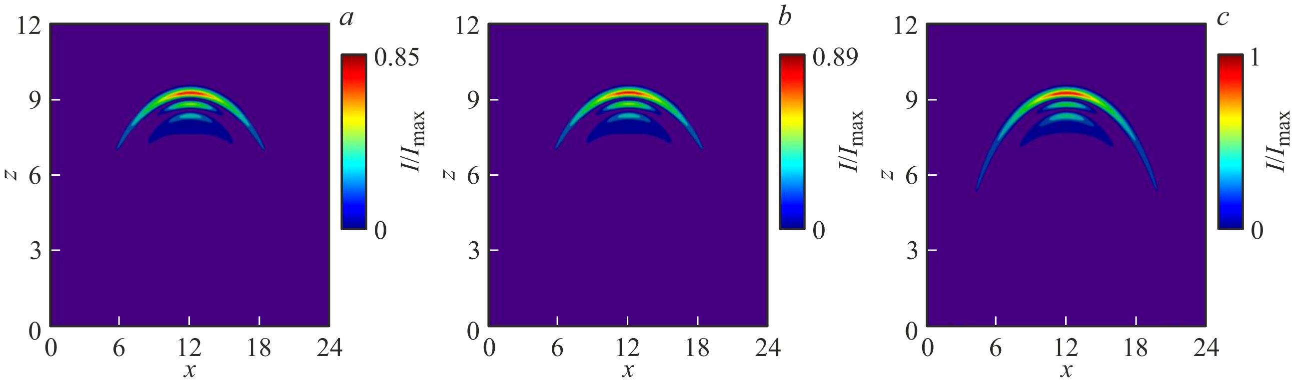

Figure 3. Intensity of the electric field of a two-dimensional electromagnetic pulse propagating through the composite with graphene nanoribbons containing metal nanoparticles at time $t = 9.0 \cdot 10^{-13}$ s for different nanoparticles: *a* — Ni; *b* — Cu; *c* — CNTs without impurities. The coordinate scales units correspond to $2 \cdot 10^{-5}$ m. The color scale represents the intensity normalized to the maximum level for all three panels (*a*–*c*).

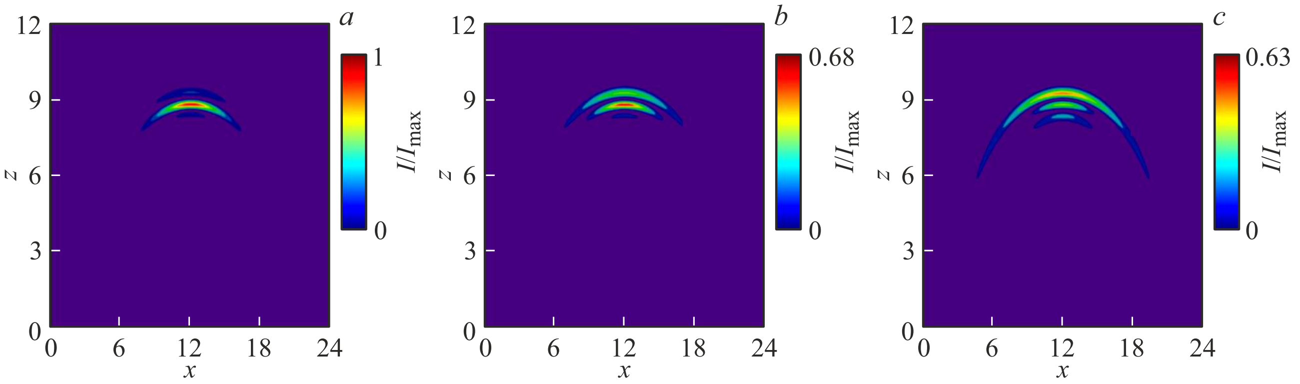

Figure 4. Intensity of the electric field of a two-dimensional electromagnetic pulse propagating through the composite with graphene nanoribbons containing Ni nanoparticles at time $t = 9.0 \cdot 10^{-13}$ s for different polymer concentrations: a — $\chi_{\text{pol}} = 0$; b — $\chi_{\text{pol}} = 0.5$; c — $\chi_{\text{pol}} = 0.8$. The coordinate scales units correspond to $2 \cdot 10^{-5}$ m. The color scale represents the intensity normalized to the maximum level at $\chi_{\text{pol}} = 0$.

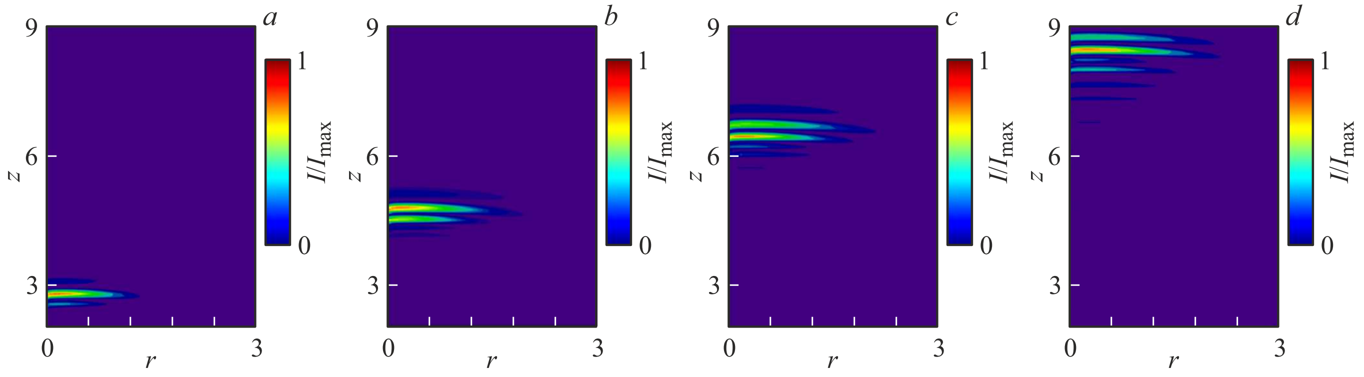

Figure 5. Intensity of the electric field of a three-dimensional electromagnetic pulse propagating through the composite with graphene nanoribbons containing nickel nanoparticles at different points in time: a — $t = 3.0 \cdot 10^{-13}$ s; b — $t = 5.0 \cdot 10^{-13}$ s; c — $t = 7.0 \cdot 10^{-13}$ s; d — $t = 9.0 \cdot 10^{-13}$ s. The coordinate scales units correspond to $2 \cdot 10^{-5}$ m. The color scale represents the intensity normalized to the maximum level for all panels (a–d).

polymer concentration affects the magnitude of the „tail“ following the pulse: the more graphene nanoribbons in the composite, the smaller the „tail.“

Conclusion

(1) A model characterizing the effect of metal nanoparticles on the dynamics of 2D and 3D electromagnetic pulses propagating in a polymer composite with graphene nanoribbons was constructed.

(2) It was demonstrated that the presence of metal nanoparticles in graphene nanoribbons in the composite material may be detected by examining the spatial and energy characteristics of a pulse.

(3) It was found that the proportion of polymer in the composite has a significant influence on the dynamics of an extremely short optical pulse. Notably, the front of a two-dimensional pulse is curved more strongly as this proportion increases. At the same time, the introduction of metal nanoparticles into the polymer composite with graphene nanoribbons allows one to suppress this effect.

(4) In the case of a three-dimensional extremely short optical pulse, the proportion of polymer in the composite was found to control the magnitude of the „tail“ moving behind the main pulse.

Acknowledgments

The author wishes to thank Prof. M.B. Belonenko for long-term support, fruitful discussions, and useful advice.

Funding

This study was carried out under state assignment of the Ministry of Science and Higher Education of the Russian Federation (project „FZUU-2023-0001“).

Conflict of interest

The author declares that she has no conflict of interest.

References

[1] P. Harris. *Carbon Nanotubes and Related Structures. New Materials for the Twenty-First Century* (Cambridge Univ. Press, 1999).

[2] N.N. Konobeeva, E.G. Fedorov, N.N. Rosanov, A.V. Zhukov, R. Bouffanais, J. Appl. Phys., **126**, 203103 (2019). DOI: 10.1063/1.5128365

[3] A. Molle, C. Grazianetti, L. Tao, D. Taneja, Md.H. Alam, D. Akinwande. Chem. Soc. Rev., **47**, 6370 (2018). DOI: 10.1039/C8CS00338F

[4] A.V. Zhukov, R. Bouffanais, N.N. Konobeeva, M.B. Belonenko. Phys. Lett. A, **380** (38), 3117 (2016). DOI: 10.1016/j.physleta.2016.07.021

[5] N.N. Konobeeva, M.B. Belonenko. Tech. Phys. Lett., **43** (4), 386 (2017). DOI: 10.1134/S106378501704023X

[6] S. Malik, J. Singh, R. Goyat, Ya. Saharan, V. Chaudhry, A. Umar, A.A. Ibrahim, S. Akbar, S. Ameen, S. Baskoutas. Heliyon, **9** (9), e19929 (2023). DOI: 10.1016/j.heliyon.2023.e19929

[7] Q.T. Phan, K.Ch. Poon, H. Sato. Intern. J. Hydrogen Energy, **46** (27), 14190 (2021). DOI: 10.1016/j.ijhydene.2021.02.006

[8] L. Shang, T. Bian, B. Zhang, D. Zhang, L.Z. Wu, C.H. Tung, Y. Yin, T. Zhang, Angew. Chem., **53**, 250 (2014). DOI: 10.1002/anie.201306863

[9] J. Huang, L. Zhang, B. Chen, N. Ji, F. Chen, Y. Zhang, Z. Zhang. Nanoscale, **2**, 2733 (2010). DOI: 10.1039/C0NR00473A

[10] A. Tavousi, M.A. Mansouri-Birjandi, M. Janfaza. Appl. Opt., **57** (20), 5800 (2018). DOI: 10.1364/AO.57.005800

[11] Y. Liu, S. Wang, H. Liu, L.-M. Peng. Nature Commun., **8**, Art. N 15649 (2017). DOI: 10.1038/ncomms15649

[12] Y. Wang, G. Sun, X. Zhang, X. Zhang, Z. Cui. Adv. Electronic Mater., **10** (10), 2400124 (2024). DOI: 10.1002/aelm.202400124

[13] S. Majumder, A. Meher, S. Moharana, K.H. Kim. Carbon, **216**, 118558 (2024). DOI: 10.1016/j.carbon.2023.118558

[14] C. Tian, W. Miao, L. Zhao, J. Wang. Rev. Phys., **10**, Art. N 100082 (2023). DOI: 10.1016/j.revip.2023.100082

[15] A.P. Johnson, C. Sabu, N.K. Swamy, A. Anto, H.V. Gangadharappa, K. Pramod. Biosens. Bioelectron., **184**, Art. N 113245 (2021). DOI: 10.1016/j.bios.2021.113245

[16] P.V. Fedotov, D.V. Rybkovskiy, I.V. Novikov, E.D. Obraztsova. Phys. Status Solidi, **259**, Art. N 2100501 (2022). DOI: 10.1002/pssb.202100501

[17] S. Jeon, P. Han, J. Jeong, W.S. Hwang, S.W. Hong. Nanomaterials, **11** (1), 33 (2021). DOI: 10.3390/nano11010033

[18] Z. Zhang, A. Fraser, S. Ye, G. Merle, J. Barralet. Nano Futur, **3**, Art. N 42003 (2019). DOI: 10.1088/2399-1984/ab4eff

[19] A.H. Castro Neto, F. Guinea, N.M.R. Peres, K.S. Novoselov, A.K. Geim. Rev. Mod. Phys., **81**, 109 (2009). DOI: 10.1103/RevModPhys.81.109

[20] R.J. Castellano, C. Aki, G. Giraldo, S. Kim, F. Fornasiero, J.W. Shan. J. Appl. Phys., **117**, 214306 (2015). DOI: 10.1063/1.4921948

[21] F. Bondino, E. Magnano, R. Ciancio, C. Castellarin Cudia, A. Barla, E. Carlino, F. Yakhou-Harris, N. Rupesinghe, C. Cepek. Phys. Chem. Chem. Phys., **19**, 32079 (2017). DOI: 10.1039/C7CP05181F

[22] D. Ürk, F.Ç. Cebeci, M.L. Öveçoğlu, H. Cebeci. Mater. Adv., **2**, 2021 (2021). DOI: 10.1039/D0MA00826E

[23] C. Zamora-Ledezma, C. Blanc, E. Anglaret. J. Phys. Chem., **116**, 13760 (2012). DOI: 10.1021/jp212113b

[24] N.N. Konobeeva. Optik, **157**, 521 (2018). DOI: 10.1016/j.ijleo.2017.11.133

[25] [E.N. Galkina, M.B. Belonenko. Opt. Spectr., **129** (10), 1280 (2021). DOI: 10.21883/EOS.2022.13.53983.1838-21

[26] S.V. Belibikhin, N.N. Konobeeva. Nanosystems: Phys., Chem., Mathem., **15** (1), 60 (2024). DOI: 10.17586/2220-8054-2024-15-1-60-64

[27] P.B. Sorokin, L.A. Chernozatonskii. Phys.-Usp., **56** (2), 105 (2013). DOI: 10.3367/UFNe.0183.201302a.0113

[28] H. Tanaka, R. Arima, M. Fukumori, D. Tanaka, R. Negishi, Y. Kobayashi, S. Kasai, T.K. Yamada, T. Ogawa. Sci. Reports, **5**, Art. N 12341 (2015). DOI: 10.1038/srep12341

[29] K. Zollner, M. Gmitra, T. Frank, J. Fabian. Phys. Rev. B, **94**, 155441 (2016). DOI: 10.1103/PhysRevB.94.155441

[30] A. Dyrda, J. Barnás. 2*D* Materials, **4**, 034003 (2017). DOI: 10.1088/2053-1583/aa7bac

[31] M. Wawrzyniak-Adamczewska. Electron. Struct., **1**, 015006 (2019). DOI: 10.1088/2516-1075/aade6

[32] G.A. Korn, T.M. Korn. *Spravochnik po matematike (dlya nauchnykh rabotnikov i inzhenerov*) (Nauka, M., 1974), pp. 43–45 (in Russian).

[33] F.G. Bass, A.A. Bulgakov, A.P. Tetervov. *Vysokochastotnye svoistva poluprovodnikov so sverkhreshetkami* (Nauka, M., 1989) (in Russian).

[34] V.A. Osipov, V.K. Fedyanin. *Rasseyanie sveta na solitonakh v poliatsetilene* (Ob”ed. Inst. Yad. Issled., Dubna, 1984) (in Russian).

[35] J.W. Thomas. *Numerical partial differential equations-finite difference methods* (Springer-Verlag, NY., 1995)

[36] A.V. Zhukov, R. Bouffanais, E.G. Fedorov, M.B. Belonenko. J. Appl. Phys., **114**, 143106 (2013). DOI: 10.1063/1.4824370

Translated by D.Safin